

# 3\_Directional\_Kinematics\_Flow\_ and\_Base.pdf

*by*

---

**Submission date:** 31-Jan-2023 01:29PM (UTC+0700)

**Submission ID:** 2003165906

**File name:** 3\_Directional\_Kinematics\_Flow\_and\_Base.pdf (1.1M)

**Word count:** 5205

**Character count:** 23874

# Directional Kinematics Flow and Base Scouring on Hybrid Engineering Structure Experimentally

H. Hendra<sup>1</sup>, M.A. Thaha<sup>2</sup>, F. Maricar<sup>3</sup>, and B. Bakri<sup>4</sup>

<sup>1</sup>Doctoral Student, Civil Engineering Department, Hasanuddin University

<sup>2</sup>Professor, Civil Engineering Department, Hasanuddin University

<sup>3</sup>Associate Professor, Civil Engineering Department, Hasanuddin University

<sup>4</sup>Associate Professor, Civil Engineering Department, Hasanuddin University

<sup>1</sup>hendra.ukit@gmail.com, <sup>2</sup>arsyad999@gmail.com, <sup>3</sup>fkmaricar@yahoo.com

<sup>4</sup>bambangbakri@gmail.com

## Abstract:

Hybrid Engineering is a technology that utilizes natural resources around the coast or river by using materials in the form of twigs or branches from mangroves which are cut and arranged to form a breakwater structure. This study aims to determine the effectiveness of hybrid engineering technology to be applied to groyne struktur to reduce longshore currents and river flow. The application of hybrid engineering as a breakwater and sediment trap in coastal areas has given good results so that it can be developed in permeable groynes.

The research was conducted experimentally in the hydraulic laboratory with physical modeling to investigation basic scouring on hybrid engineering structures with several model scenarios by changing the characteristics of brushwood structure in the form of density or permeability and finding variables that significantly affect base scouring, namely velocity (V), water level (h), structure length (B) and grain size sediment (d50) as well as analyzing the relationship between these parameters so that a dimensionless parameter formula is found that is used to describe the relationship. To obtain the relationship between the influential parameter and depth scouring (ds), a dimensionless parameter of relative depth scouring ds/B is used for several influencing parameters. The results obtained are that the relative depth scouring (ds/B) will be greater because it is influenced by the smaller the permeability ratio of the structure and the larger the diameter of the sediment grains.

**Keywords:** Hybrid Engineering, permeability, longshore current, river flow, depth scouring

## I. INTRODUCTION

Handling coastal and river flow problems by using large investments or hard structures is carried out as a response to changes that occur on the coast and river. Hard and massive traditional infrastructure, still like a breakwater, is one solution that is often used in efforts to solve problems. However, these structures are expensive and often prove counterproductive on muddy shores. In addition, handling using hard structures cannot restore lost mangrove belts.

To protect the coastline from erosion caused by longshore currents, mangrove buffer zones must be created. The necessary first step is to stop the erosion process by returning lost

sediments so as to obtain a stable shoreline. This approach is called hybrid engineering. (HE) in this case engineering techniques are combined with existing processes in nature and available resources, resulting in dynamic solutions that are able to adapt to changing circumstances. The HE structure approach can be applied in various situations and ecosystems. The HE structure in the form of a Permeable Breakwater is carried out by utilizing natural resources around the coast using materials in the form of twigs or branches from mangroves which are cut and arranged to form a breakwater. Apart from using twigs or mangrove branches, materials such as bamboo, which is an industrial plant that can be cultivated, can also be used, so that the amount is quite large when applied to coastal areas.

To deal with abrasion caused by longshore currents, it is necessary to build perpendicular buildings or groynes which are useful for protecting beaches that are threatened with erosion by partially blocking longshore sediment transport (littoral drift) to balance sediment input-output so that the rate of sediment transport in the updrift zone will be reduced. increases and conversely the rate of sediment transport in the downdrift zone will decrease.

The purpose of this study is to examine how HE structure are applied to permeable groins which function to reduce longshore currents and restore sediment balance.

The results of this study are expected to make groyn permeable an alternative beach safety for muddy areas that are environmentally friendly, especially from the raw materials in the form of twigs, tree trunks or bamboo which can be obtained from areas around the coast and can be carried out independently by fishermen or local residents coastal areas on muddy coasts to restore water conditions

The purpose of this study is how to identify the variables that influence depth scouring (ds) and permeability ( $\zeta$ ) including the magnitude of each effect, how to analyze and obtain the relationship between variables that influence the parameters studied, how to measure the effectiveness of the structure through the value efficiency obtained. The goal to be achieved in this study is to find and recognize the variables that affect depth scour (ds) and permeability ( $\zeta$ ) so that an effective and efficient structural design is obtained to reduce direct currents or longshore currents.

## II. MATERIALS AND METHODOLOGY

The type of research used is Experimental, where the conditions are created and regulated by the researcher with the aim of analyzing the relationship between parameters that influence the research. In this study, two sources of data were used, namely: Primary data is data obtained directly from a physical model simulation in the laboratory. Secondary Data is data obtained from the literature and the results of existing studies that have been carried out both in the laboratory and in the laboratory carried out in other places related to local scour research at the bottom of the structure.

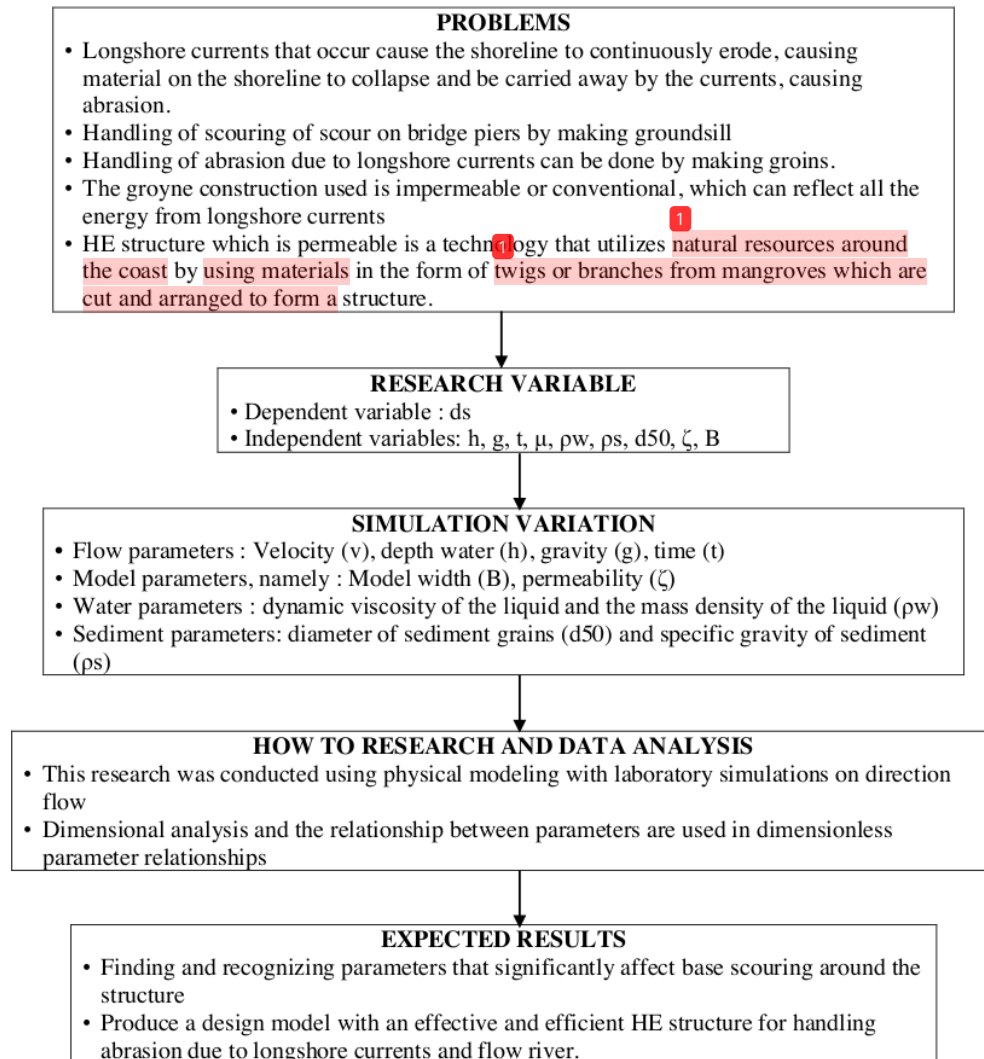
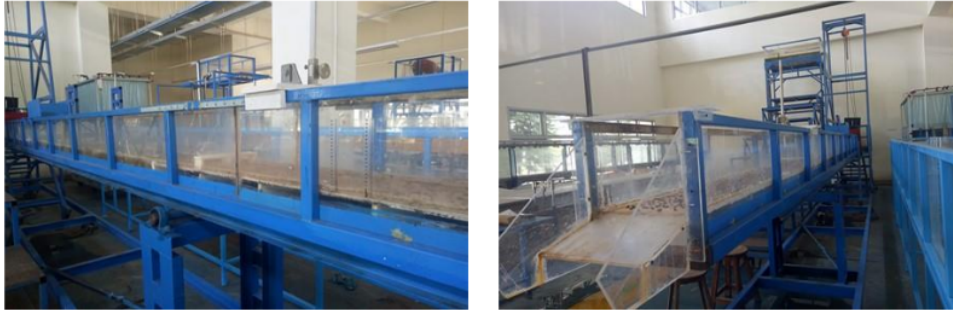


Fig. 2 : Research Framework

## 2.1 Materials and tools

The model is made of round planed wood with a diameter of 5 mm which is assembled and arranged with a height of 20 cm and a width of 30 cm using a frame. The wood is arranged in an impermeable horizontal direction and a vertical direction permeable with a spacing of 2 mm, 5 mm and 10 mm.



**Fig 3 :** Flume test model used



**Fig. 4 :** In-flume structure HE structure model

## 2.2 Running of simulation

Based on the considerations of the facilities in the laboratory, the materials available and the accuracy when making measurements, the model is made with perfect geometric congruence (non-distortion) and dynamic congruence according to the conditions of the Froude number. The model scale in this study used a model scale of 1: 10, the full model scale values are shown in Table 1.

**Tabel 1.** Research Model Scale

Variable	Symbol	Scale
Height Scale	$n_H$	1:10
Length Scale	$n_L$	1:10
Depth Water scale	$n_h$	1:10
Velocity Scale	$n_v$	1:10

Preparation for the initial simulation on the flume (without a structural model), to obtain initial data, namely:

1. The slope of the flume used in this study to determine the flow velocity, the slope of the glass channel used is 0.00005, 0.0028 and 0.012, the velocity is measured at every 200 mm distance along 2000 mm
2. Speed is measured using a digital current meter at every distance of 200 mm along 2000 mm,
3. Each speed measurement is carried out 3 times for the horizontal direction and 3 times for the vertical direction (0.2d, 0.6d, 0.8d)
3. Starting the simulation of flow velocity and head height without a model by flowing water that has been adjusted for discharge. This simulation is carried out to ensure that the flow height and velocity in the glass channel are in accordance with the variations that have been determined in this study.
4. Calibrate the tool with a simulation without a model by checking the flow velocity with the discharge that comes out.
5. Place the test model in the middle of the glass channel
7. After all the components are ready, the flow velocity simulation begins by flowing the flow into the glass channel as in procedure no. 2 and no. 3
8. Measure and record the speed in front of the model and behind the model
9. Measuring the depth of scour in each segment by taking 7 point data for each segment after the first 10 minutes, then the second 10 minutes and the third 10 minutes.
10. Perform variations in speed, permeability models, and sediment grains

### 2.3 Research Parameters

The dependent parameter in this study is depth scour ( $d_s$ ) which will be influenced by several other parameters related to local scour. The independent parameters used in this study are;  $v$ ,  $h$ ,  $g$ ,  $t$ ,  $\mu$ ,  $\rho_w$ ,  $\rho_s$ ,  $d_{50}$ ,  $\zeta$ ,  $P$  with the function of each of the free parameters namely; Flow parameters are: velocity ( $v$ ), depth water ( $h$ ), acceleration due to gravity ( $g$ ) and time ( $t$ ). Model parameters, namely: model width ( $B$ ), permeability ( $\zeta$ ), water parameters, namely: dynamic viscosity of liquid and mass density of liquid ( $\rho_w$ ) Sediment parameters, namely: sediment grain diameter ( $d_{50}$ ) and specific gravity sediment ( $\rho_s$ ).

In this study, the data were analyzed with various relationships between parameters and then it could be determined based on the relationships between parameters expressed in dimensionless numbers using the Langhaar method. This method was chosen with the consideration that relatively few influential variables, so this method is considered more appropriate.

**Table 2.** Specific model of HE structure

Property	Details
Material of HE structure	Dowels wood
Wood diameter	14 mm
Tall structure	20 cm
Wide structure	30 cm
Length structure 1	10 cm
Length structure 1	20 cm
Permeability distance 1 (P1)	2 mm
Permeability distance 2 (P2)	5 mm
Permeability distance 3 (P3)	10 mm
Frame of structure	Iron

## 2.5 Longshore current

Coast currents are the movement of water vertically or horizontally caused by several factors such as wind, salinity, density differences and others. Currents in shallow waters or around the coast are longshore currents and crossshore currents. Longshore Current is an ocean current that is parallel to the shoreline. These currents can shape the coastline to meander. Longshore currents occur between the breaking wave area and the shoreline, where when the incoming waves form an oblique angle with the breaking shoreline, longshore currents occur due to the momentum flux gradient in the surf zone area.

Longshore currents have a relatively small speed, averaging 0.3 m/sec. Although these longshore currents generally have low speeds, they greatly affect littoral transport processes because they move along the coast for a long time and continuously as long as there are waves so as to be able to move sediment, it is necessary to discuss the longshore current velocity as the driving force.

## 2.6 Depth Scouring

Depth scour under the structure is one of the phenomena that many coastal structures experience when attacked by waves, currents or a combination of both. This has been recognized as one of the factors causing the failure of coastal structures.

The depth scour process is caused by an increase in the mass transport capacity of the base material leaving its initial location under the structure. This is due to the effect of increasing the intensity of the flow around the toe of the structure by considering the longshore current velocity as a causative factor.

## III. DATA ANALYSIS AND INTERPRETATION

### 3.1 Velocity Data Validation

In this study the discharge used is fixed so that the flow velocity is determined based on the slope of the glass channel. The results of speed measurements on each slope condition are then validated using the Manning equation:

$$v = \frac{1}{n} R^{2/3} I^{1/2} \dots\dots\dots (1)$$

**Table 3.** Flow velocity data calibration from measurement results with speed using the Manning equation

Segment	STA	I = 0.00005		I = 0.0028		I = 0.012	
		v measure	v count	v measure	v count	v measure	v count
A	0	18.35	18.38	20.76	20.63	42.91	43.18
B	20	18.22	18.36	20.63	20.72	43.00	43.36
C	40	18.45	18.36	20.72	20.73	43.00	43.29
D	60	18.23	18.47	20.81	20.76	42.85	43.30
E	80	18.39	18.43	20.74	20.79	43.29	43.47
F	100	18.24	18.48	20.74	20.87	44.00	43.77
G	120	18.28	18.41	20.51	20.88	44.25	43.92
H	140	18.24	18.40	20.50	20.79	43.58	43.42
I	160	18.37	18.36	20.98	20.84	43.52	43.69
J	180	18.39	18.34	21.03	20.91	43.12	43.39

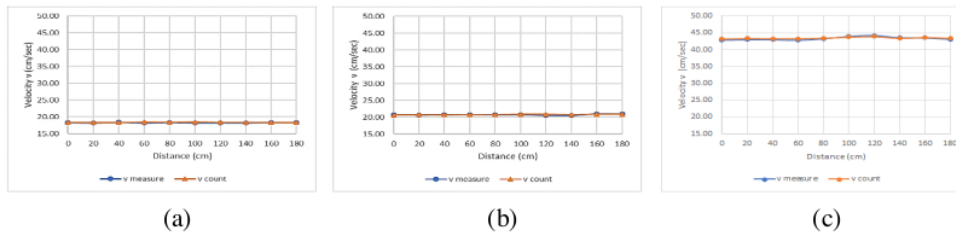


**Fig. 5 :** Velocity data from measurement results and Manning's equation, (a) on slope 0.00005 (b) on slope 0.0028, (c) on slope 0.012

### 3.1 Flow Velocity Change

Changes in current velocity are obtained by calculating the ratio of current velocity before the structure and current velocity after the structure, where the structure is located at a distance of 80 cm.

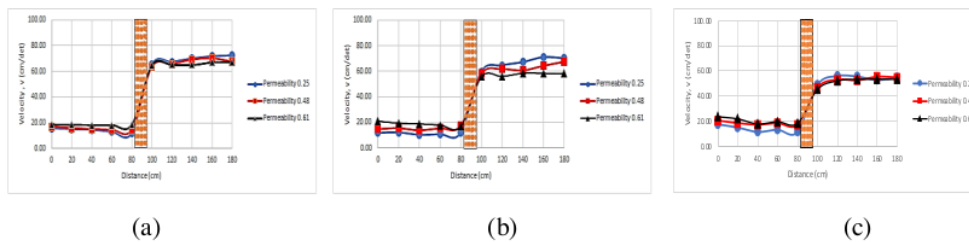


**Fig. 6 :** Changes in flow velocity, (a) at a slope of 0.00005 (b) at a slope of 0.0028, (c) at a slope of 0.012

The relationship between permeability in the HE structure model and changes in current velocity is shown in Figure 6a, which shows an increase in current velocity after modeling. In the model with a permeability of 0.61 with an initial speed of 18 cm/s it becomes 67 cm/s after

the model, in a model with a permeability of 0.48 with an initial speed of 17 cm/s it becomes 67 cm/s after the model and in a model with a permeability of 0.25 the initial speed is 16 cm/s sec to 72 cm/s after model.

The relationship between porosity in the HE structure model and changes in current velocity on a slope of 0.0028 is shown in Figure 6b, in a model with a permeability of 0.61 with an initial speed of 20.83 cm/s it becomes 62.36 cm/sec after modeling, in a model with a permeability of 0.48 the initial speed becomes 24.11 cm /sec after the model becomes 69.70 cm/sec and in a model with a permeability of 0.25 the initial speed is 11.93 cm/sec becomes 70.30 cm/sec after the model.

The relationship between porosity in the HE structure model and changes in current velocity at a slope of 0.012 is shown in Figure 6c, which shows an increase in current velocity after modeling. In the model with a permeability of 0.61 the initial speed of 33.80 cm/s becomes after the model 66.47 cm/sec, in the permeability model of 0.48 the initial speed of 20.64 cm/sec becomes 59.81 after the model and in the model with a permeability of 0.25 the initial speed of 17.84 cm/sec becomes 45.16 cm /s after the model.

### 3.2 Sediment Grain Size Analysis

Sediment grain analysis is intended to determine the type of sediment material based on grain diameter. The grain size classification used in this study is according to AGU (American Geophysical Union). Sediment material grains used are 3 types (coarse, medium and fine), based on the results of the Gradation test Sediment material grains are converted into a grain size diameter chart as shown in Figure 7.

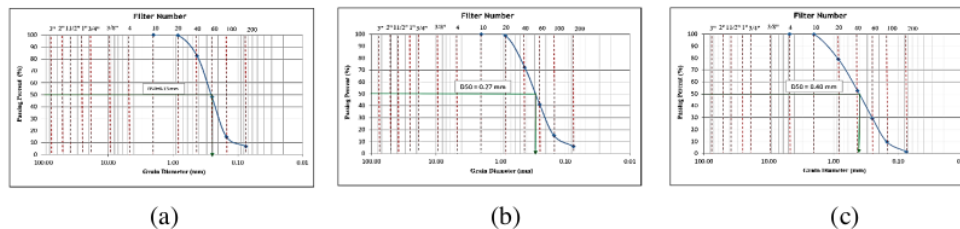


**Fig. 7** : Gradation test of sediment grains on three types of sediment, (a) sediment with a specific gravity of 2.71 gr/cm<sup>3</sup> (b) sediment with a specific gravity of 2.79 gr/cm<sup>3</sup>, (c) sediment with a specific gravity of 2.80 gr/cm<sup>3</sup>

From the results of the gradation test, the grain diameter of the sediment (d<sub>50</sub>) was obtained for fine sediment Figure 5a obtained a value of 0.13 mm, for moderate sediment d<sub>50</sub> obtained a value of 0.27 mm and for coarse sediment d<sub>50</sub> obtained a value of 0.40 mm.

### 3.3 Dimensional Analysis of Research Parameter

Dimensional analysis in this study used the Langhaar method. This method was chosen with the consideration that relatively few influential variables, so this method is considered more appropriate. The basic equation obtained is :

$$\pi_1 = \frac{ds}{h}; \pi_2 = \frac{v}{\sqrt{g \cdot h}}; \pi_3 = \frac{B}{h}; \pi_4 = \frac{h}{\sqrt{g \cdot t^2}}; \pi_5 = \frac{\rho_w \cdot h^{2.5} \cdot \sqrt{g}}{\mu}; \pi_6 = \frac{\rho_s \cdot h^{2.5} \cdot \sqrt{g}}{\mu}; \pi_7 = \frac{d_{50}}{h}; \pi_8 = \zeta$$

Where :

ds	: depth scouring	$\rho_w$	: specific gravity of water
h	: height water level	$\rho_s$	: specific gravity of sediment
g	: gravity	$\mu$	: liquid viscosity
B	: length of model structure HE	$d_{50}$	: grain size sediment
t	: time	$\zeta$	: permeability of model structure HE

Furthermore, these parameters can be combined to get another dimensionless number, namely:

$$\pi_9 = \pi_1 \times \frac{1}{\pi_3} = \frac{ds}{h} \times \frac{h}{B} = \frac{ds}{B};$$

$$\pi_{10} = \pi_7 \times \pi_2 = \frac{d_{50}}{h} \times \frac{v}{\sqrt{g \cdot h}} = \frac{d_{50} \cdot v}{h^2};$$

$$\pi_{11} = \pi_5 \times \frac{1}{\pi_6} = \frac{\rho_w \cdot h^{2.5} \cdot \sqrt{g}}{\mu} \times \frac{\mu}{\rho_s \cdot h^{2.5} \cdot \sqrt{g}} = \frac{\rho_w}{\rho_s}$$

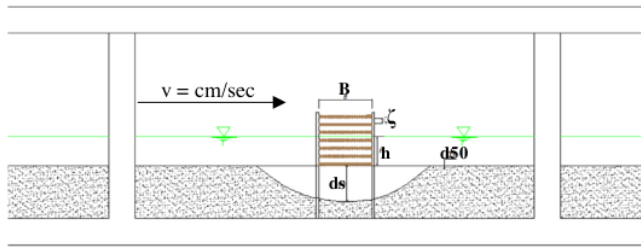


**Fig. 8** : Schematic base scouring of the structure HE in the flume test

Depth scouring (figure 8) can be written as a function of the listed parameters, which also appear in equation :

The dimensionless numbers used in this study are  $\pi_2, \pi_4, \pi_7, \pi_8, \pi_{11}$ , mathematically the depth scouring coefficient produced in this study is a function of the following parameters:

$$\frac{ds}{B} = f \left[ \frac{v}{\sqrt{g \cdot h}}; \frac{h}{\sqrt{g \cdot t^2}}; \frac{d_{50}}{h}; \frac{\rho_s}{\rho_w}; \zeta \right]$$

Where  $ds/h$  is relative depth scouring,  $v/\sqrt{g \cdot h}$  is froude number,  $B/h$  is relative model length,  $d_{50}/h$  is relative sediment grain size diameter,  $\zeta$  is model permeability

### 3.4 Effect of froude number ( $v/\sqrt{g \cdot h}$ ) on relative depth scouring ( $ds/B$ )

Figure 9 - 11 shows the relationship between the parameter froude number  $v/\sqrt{g \cdot h}$  which is related to the relative depth scouring ( $ds/B$ ) that the greater the value of the froude number  $v/\sqrt{g \cdot h}$ , the smaller the depth scouring will be in all models with permeability. This is because the larger cavity has a larger cavity area so that the scour will be smaller because of the wider

frictional area, thus the energy dissipated is greater. Variations are made on the height of the cavity and the length of the structure.

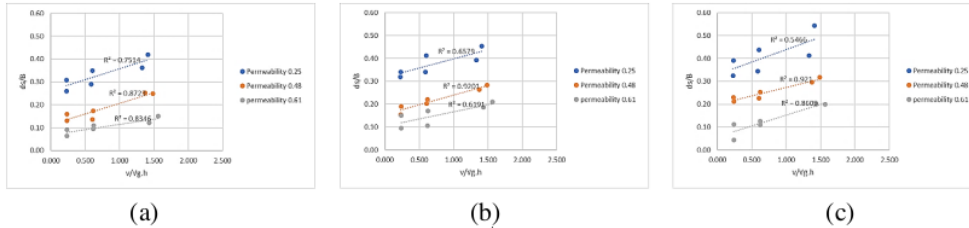


**Fig. 9 :** (a) Relationship between  $ds/B$  and  $v/\sqrt{gh}$  at  $t_1$  (10 minutes), (b) Relationship between  $ds/b$  and  $v/\sqrt{gh}$  at  $t_2$  (20 minutes) (c) The relationship between  $ds/b$  and  $v/\sqrt{gh}$  at  $t_3$  (30 minutes) at  $d50/\rho_s = 0.14$

Figure 9 shows the relationship between the froude number  $v/\sqrt{g.h}$  and the relative depth scouring  $ds/B$  at  $d50/\rho_s = 0.14$  for a permeability of 0.25 at  $t_1$  (10 minutes) resulting in a  $ds/B$  value of 0.26 – 0.36, at  $t_2$  (20 minutes) resulting in a  $ds/B$  value of 0.32 – 0.45 and at  $t_3$  (30 minutes) produces a  $ds/B$  value of 0.33 – 0.54, permeability of 0.48 at  $t_1$  (10 minutes) produces a  $ds/B$  value of 0.21 – 0.35, at  $t_2$  (20 minutes) produces a  $ds/B$  value of 0.23 – 0.37 and at  $t_3$  (30 minutes) produces a  $ds/B$  value of 0.27 – 0.43, permeability of 0.61 at  $t_1$  (10 minutes) produces a  $ds/B$  value of 0.05 – 0.12, at  $t_2$  (20 minutes) produces a  $ds/B$  value of 0.05 – 0.17 and at  $t_3$  (30 minutes) produces a depth scouring of 0.05 – 0.18. The froude number  $v/\sqrt{g.h}$  has a significant effect on the  $ds/B$  parameter, the higher the froude number the smaller the depth scouring that occurs.

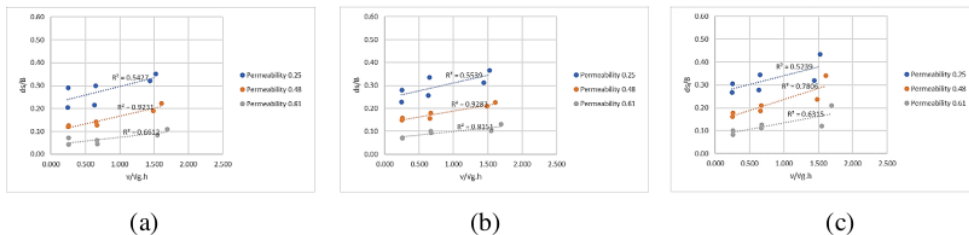


**Fig. 10 :** (a) Relationship between  $ds/b$  and  $v/\sqrt{gh}$  at  $t_1$  (10 minutes), (b) Relationship between  $ds/b$  and  $v/\sqrt{gh}$  at  $t_2$  (20 minutes), (c) The relationship between  $ds/b$  and  $v/\sqrt{gh}$  at  $t_3$  (30 minutes) at  $d50/\rho_s = 0.10$

Figure 10 shows the froude number  $v/\sqrt{g.h}$  on  $d50/\rho_s = 0.10$  in the range of 0.25 – 1.55 with a relative depth scouring ( $ds/B$ ) for a permeability of 0.25 at  $t_1$  (10 minutes) resulting in a  $ds/B$  value of 0.21 – 0.35, at  $t_2$  (20 minutes) produces a  $ds/B$  value of 0.23 – 0.37 and at  $t_3$  (30 minutes) produces a  $ds/B$  value of 0.27 – 0.43, permeability 0.48 at  $t_1$  (10 minutes) produces a  $ds/B$  value of 0.12 – 0.22, at  $t_2$  (20 minutes) produces a  $ds/B$  value of 0.15 – 0.21 and at  $t_3$  (30 minutes) produces a  $ds/B$  value of 0.16 – 0.24, permeability of 0.61 at  $t_1$  (10 minutes) results in a  $ds/B$  value of 0.04 – 0.11, at  $t_2$  (20 minutes) produces a  $ds/B$  value of 0.07

– 0.13 and at t3 (30 minutes) resulting in a ds/B value of 0.08 – 0.21. The parameter  $v/\sqrt{gh}$  has a significant effect, the higher the froude number the smaller the depth scouring that occurs.

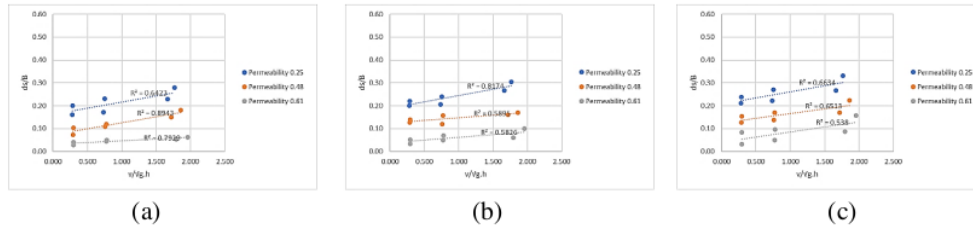


**Fig. 11 :** (a) Relationship between ds/b and  $v/\sqrt{gh}$  at t1 (10 minutes), (b) Relationship between ds/b and  $v/\sqrt{gh}$  at t2 (20 minutes) (c) The relationship between ds/b and  $v/\sqrt{gh}$  at t3 (30 minutes) at  $d50/\rho_s = 0.05$

3

Figure 11 shows the froude number  $v/\sqrt{gh}$  on a slope of 0.012 in the range 0.29 – 1.67 with a relative depth scouring (ds/B) for a permeability of 0.2 at t1 (10 minutes) resulting in a ds/B value of 0.16 – 0.28, at t2 (20 minutes) produces a ds/B value of 0.20 – 0.31 and at t3 (30 minutes) produces a ds/B value of 0.21 – 0.33, permeability 0.48 at t1 (10 minutes) produces a depth scouring of 0.07 – 0.15, at t2 (20 minutes) produces a ds/B value of 0.12 – 0.17 and at t3 (30 minutes) produces a ds/B value of 0.13 – 0.22, permeability of 0.61 at t1 (10 minutes) produces a ds/B value of 0.03 – 0.10, at t2 (20 minutes) produces a ds/B value of 0.03 – 0.10 and at t3 (30 minutes) resulting in a ds/B value of 0.03 – 0.16. The parameter  $v/\sqrt{gh}$  has a significant effect, the higher the froude number the smaller the depth scouring that occurs. Structures with a permeability of 0.61 depth scouring that occurs at times t1, t2 and t3 are not significantly different.

### 3.5 Effect of relative sediment grain diameter (d50/h) on relative depth scouring (ds/B)

Figure 12-14 shows the effect of d50/h relative sediment grain diameter on the relative depth scouring ds/B. The figures in Fig. 12-14 show a clear trend of relative grain diameter d50/h with increasing depth scouring with increasing permeability of the HE structure.

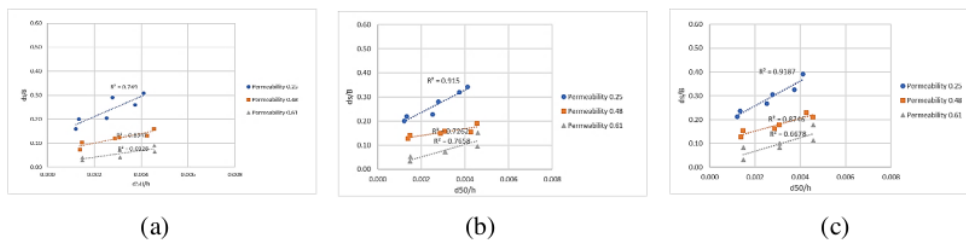


**Fig. 12 :** (a) Relationship between d50/h and ds/B at t1 (10 minutes), (b) Relationship between d50/h and ds/B at t2 (20 minutes) (c) Relationship d50/h with ds/B at t3 (30 minutes) at a slope of 0.00005

Figure 12 shows the relationship between the grain size of the sediment d50/h and the relative depth scouring relative (ds/B) at a slope of 0.00005 for a permeability of 0.25 at t1 (10

minutes) resulting in a  $ds/B$  value of 0.16 – 0.31, at  $t_2$  (20 minutes) resulting in a  $ds/B$  value of 0.20 – 0.34 and at  $t_3$  (30 minutes) produces a  $ds/B$  value of 0.21 – 0.34, permeability of 0.48 at  $t_1$  (10 minutes) results in a  $ds/B$  value of 0.12 – 0.16, at  $t_2$  (20 minutes) produces a  $ds/B$  value of 0.13 – 0.19 and at  $t_3$  (30 minutes) produces a  $ds/B$  value of 0.14 – 0.23, permeability of 0.61 at  $t_1$  (10 minutes) produces a  $ds/B$  value of 0.03 – 0.11, at  $t_2$  (20 minutes) produces a  $ds/B$  value of 0.05 – 0.17 and at  $t_3$  (30 minutes) produces a  $ds/B$  value of 0.05 – 0.18. The effect of relative sediment grain diameter  $d_{50}/h$  affects the  $ds/B$  parameter fairly evenly for each permeability, the larger the sediment grain diameter the greater the depth scouring that occurs.

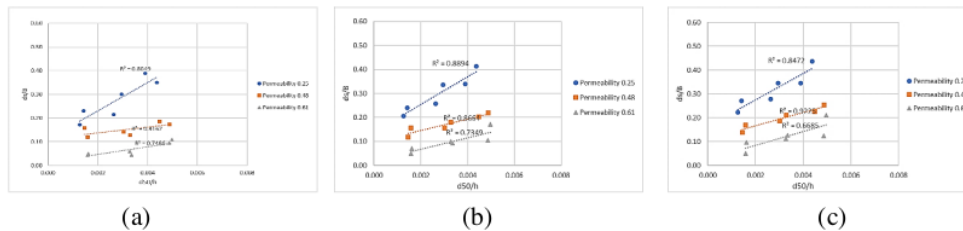


**Fig. 13 :** (a) Relationship between  $d_{50}/h$  and  $ds/B$  at  $t_1$  (10 minutes), (b) Relationship between  $d_{50}/h$  and  $ds/B$  at  $t_2$  (20 minutes), (c) The relationship between  $d_{50}/h$  and  $ds/B$  at  $t_3$  (30 minutes) at a slope of 0.0028

Figure 13 shows the relationship between the grain size of the sediment  $d_{50}/h$  and the relative depth scouring  $ds/B$  at a slope of 0.0028 for a permeability of 0.25 at  $t_1$  (10 minutes) resulting in a  $ds/B$  value of 0.21 – 0.35, at  $t_2$  (20 minutes) resulting in a  $ds/B$  value of 0.20 – 0.34 and at  $t_3$  (30 minutes) produces a  $ds/B$  value of 0.21 – 0.40, permeability of 0.48 at  $t_1$  (10 minutes) results in a  $ds/B$  value of 0.17 – 0.42, at  $t_2$  (20 minutes) produces a  $ds/B$  value of 0.13 – 0.19 and at  $t_3$  (30 minutes) produces a  $ds/B$  value of 0.14 – 0.23, permeability of 0.61 at  $t_1$  (10 minutes) produces a  $ds/B$  value of 0.04 – 0.14, at  $t_2$  (20 minutes) produces a depth scouring of 0.05 – 0.17 and at  $t_3$  (30 minutes) produces a  $ds/B$  value of 0.04 – 0.12. The relative sediment grain diameter  $d_{50}/h$  has a significant effect on the  $ds/B$  parameter at a permeability of 0.25, the larger the sediment grain diameter the greater the depth scouring that occurs.

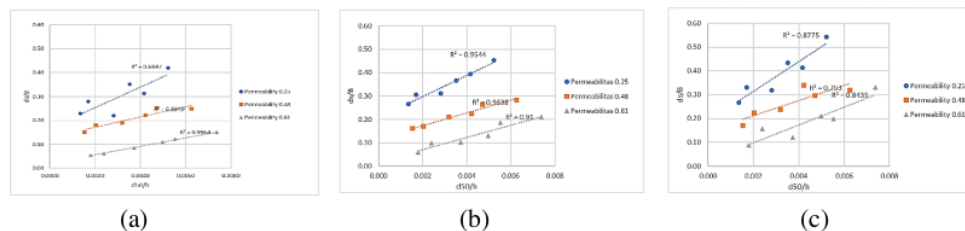


**Fig. 14 :** (a) Relationship between  $d_{50}/h$  and  $ds/B$  at  $t_1$  (10 minutes), (b) Relationship between  $d_{50}/h$  and  $ds/B$  at  $t_2$  (20 minutes), (c) Relationship  $d_{50}/h$  with  $ds/B$  at  $t_3$  (30 minutes) at a slope of 0.012

Figure 14 shows the effect of sediment grain diameter with relative depth scouring ( $ds/B$ ) for a permeability of 0.2 at  $t_1$  (10 minutes) resulting in a  $ds/B$  value of 0.23 – 0.35, at  $t_2$  (20 minutes) resulting in a  $ds/B$  value of 0.27 – 0.41 and at  $t_3$  (30 minutes) produces a  $ds/B$  value

of 0.22 – 0.47, permeability of 0.48 at t1 (10 minutes) produces a ds/B value of 0.18 – 0.25 , at t2 (20 minutes) produces a ds/B value of 0.16 – 0.28 and at t3 (30 minutes) produces a ds/B value 0.16 – 0.35, 0.61 permeability at t1 (10 minutes) produces a ds/B value of 0.05 – 0.15, at t2 (20 minutes) produces a ds/B value 0.06 – 0.16 and at t3 (30 minutes) produces a ds/B value 0.06 – 0.21 ds/B value. The d50/h parameter has a significant effect, the larger the grain diameter, the greater the depth scouring that occurs.

#### IV. CONCLUSION

The parameters that greatly influence the damage to the HE structure model are obtained by the Langhaar method. The use of HE structure can be considered with the relative depth scouring ds/B that occurs in HE structure which will be greater if the froude number is greater. The relative sediment grain diameter factor d50/h also affects the relative depth scouring ds/B because the larger the sediment grain diameter the greater the depth scouring that occurs.

#### REFERENCES

- [1] De Vriend HJ, v. K. 2012. Building with Nature: Thinking, acting and interacting differently. Ecoshape. The Netherlands: Building with Nature
- [2] Dean, R. G. a. Dalrymple, 1984, Water Waves Mechanics for Engineer and Scientist, Prentice Hall, Inc., New Jersey; Englewood Cliffs.
- [3] Juventus W. R. Ginting, 2018, Efficiency of Physical Model of Absorbing Wave Energy with Permeable Breakwater, Hydraulic Engineering Journal Vol. 9 No. 1
- [4] M.A Thaha, 2001. Konservasi Energi Gelombang Melalui Rumpun Bakau (Rhizophora sp), Universitas Gadjah Mada. Yogyakarta
- [5] Pallu, M.S., 2011. Sedimen Transport. Teknik Sipil Universitas Hasanuddin
- [6] Siry, H. Y. 2018, Struktur Hybrid Engineering – Ecosystem-Based Engineering Solutions for Coastal Area Restoration, Marine and Fisheries Ministry
- [7] Tonneijck, F. W. 2015. Building with Nature Indonesia Securing Eroding Delta Coastlines. R1.5\_R1.6 Design & Engineering plan incl. Hardware plan. Nedherland: Ecoshape
- [8] Triatmodjo, B., 1999. Costal Engineering Book. Beta Offset. Yogyakarta
- [9] Weka Mahardi, 2014, Study of the Effectiveness of the Method of Structural Breakwater and Hybrid-Engineering Permeable Structures as a Study of the Development of the Beach Rehabilitation Concept in Demak Regency. Thesis Indonesia University, Jakarta.
- [10] Yuwono, Nur. 1996. Hydraulic Modelling. Hydraulic and Hydrology Laboratory, Center for Inter-University of Engineering Sciences – Gajah Mada University. Yogyakarta

# 3\_Directional\_Kinematics\_Flow\_and\_Base.pdf

## ORIGINALITY REPORT

**11** %  
SIMILARITY INDEX

**1** %  
INTERNET SOURCES

**10** %  
PUBLICATIONS

**3** %  
STUDENT PAPERS

## PRIMARY SOURCES

**1** H Hafid, M A Thaha, F Maricar, B Bakri. "Hybrid engineering on permeable groins to reduce the longshore current", IOP Conference Series: Earth and Environmental Science, 2021 **6** %  
Publication

**2** Submitted to Kwansei Gakuin University **2** %  
Student Paper

**3** J. E. Simpson. "The dynamics of the head of a gravity current advancing over a horizontal surface", Journal of Fluid Mechanics, 10/1979 **1** %  
Publication

**4** R Bachrun, M S Pallu, M A Thaha, B Bakri. "Effect of water discharge variation on water levels and flow characteristics in pipeline networks", IOP Conference Series: Earth and Environmental Science, 2020 **<1** %  
Publication

**5** Nini H Aswad, Herman Parung, Rita Irmawaty, A Arwin Amiruddin. "The Effects of Reduced **<1** %

# Beam Section on Castellated Beam", MATEC Web of Conferences, 2017

Publication

---

6	"Abstracts", International Journal of Stroke, 2008 Publication	<1 %
7	Advances in Water Resources and Hydraulic Engineering, 2009. Publication	<1 %
8	es.scribd.com Internet Source	<1 %
9	Rupal H. Trivedi, M. Edward Wilson, Luanna R. Bartholomew. "Extensibility and scanning electron microscopy evaluation of 5 pediatric anterior capsulotomy techniques in a porcine model", Journal of Cataract & Refractive Surgery, 2006 Publication	<1 %
10	Submitted to University of Newcastle Student Paper	<1 %
11	ejournal.uika-bogor.ac.id Internet Source	<1 %
12	ijettjournal.org Internet Source	<1 %
13	"Stormwater Management for Smart Growth", Springer Science and Business Media LLC,	<1 %

2005

Publication

---

14

[www.bartleby.com](http://www.bartleby.com)

Internet Source

<1 %

---

Exclude quotes  On

Exclude matches  < 5 words

Exclude bibliography  On